Communication in a Poisson Field of Interferers–Part II: Channel Capacity and Interference Spectrum

Pedro C. Pinto, *Student Member, IEEE,* and Moe Z. Win, *Fellow, IEEE*

***Abstract*—In Part I of this paper, we presented a mathematical model for communication subject to both network interference and noise, where the interferers are scattered according to a spatial Poisson process, and are operating asynchronously in a wireless environment subject to path loss, shadowing, and multipath fading. We determined the distribution of the aggregate interference and the error performance of the link. In this second part, we characterize the capacity of the link subject to both network interference and noise. Then, we put forth the concept of *spectral outage probability* (SOP), a new characterization of the aggregate radio-frequency emission generated by communicating nodes in a wireless network. We present some applications of the SOP, namely the establishment of spectral regulations and the design of covert military networks. The proposed framework captures all the essential physical parameters that affect the aggregate network emission, yet is simple enough to provide insights that may be of value in the design and deployment of wireless networks.**

***Index Terms*—Stochastic geometry, Poisson field, aggregate network emission, channel capacity, spectral outage, stable laws.**

I. Introduction

THE application of the spatial Poisson process to cellular networks was investigated in [1], and later advanced in [2]–[4]. However, these studies focus mostly on error performance metrics, and do not attempt a characterization of the channel capacity and interference spectrum. Furthermore, they often ignore random propagation effects (e.g. shadowing and fading) [1]; assume perfect synchronization between different interferers at the symbol or slot level [3]; or restrict the node locations to a disk in the two-dimensional plane [4], [5], which complicates the analysis and provides limited insights into the effect of network interference. In [6], [7], the authors analyze coexistence issues in narrowband and ultrawideband networks, but consider only a small, fixed number of interferers.

Manuscript received November 16, 2007; accepted March 18, 2008. The associate editor coordinating the review of this paper and approving it for publication was D. Dardari.

This research was supported, in part, by the Portuguese Science and Technology Foundation under grant SFRH-BD-17388-2004; the MIT Institute for Soldier Nanotechnologies; the Office of Naval Research under Presidential Early Career Award for Scientists and Engineers (PECASE) N00014-09-1-0435; and the National Science Foundation under grant ECS-0636519. This paper was presented, in part, at the IEEE Global Telecommunications Conference, San Francisco, CA, November 2006.

P. C. Pinto and M. Z. Win are with the Laboratory for Information and Decision Systems (LIDS), Massachusetts Institute of Technology, Room 32-D674, 77 Massachusetts Avenue, Cambridge, MA 02139, USA (e-mail: {ppinto, moewin}@mit.edu).

Digital Object Identifier 10.1109/TWC.2010.07.071283

In Part I of this paper [8], we introduced a framework where the interferers are scattered according to a spatial Poisson process, and are operating asynchronously in a wireless environment subject to path loss, shadowing, and multipath fading. Under this scenario, we determined the statistical distribution of the aggregate interference, and the corresponding error performance of the link. In this second part, we characterize the capacity of the link subject to both network interference and noise. Then, we put forth the concept of spectral outage probability (SOP), a new characterization of the aggregate radio-frequency (RF) emission generated by communicating nodes in a wireless network. Lastly, we quantify these metrics as a function of important system parameters, such as the signal-to-noise ratio (SNR), interference-to-noise ratio (INR), path loss exponent of the channel, and spatial density of the interferers. Our analysis easily accounts for all the essential physical parameters that affect the aggregate network emission. Furthermore, the concept of SOP can be used (e.g., in commercial or military applications) to evaluate and limit the impact of network interference on any given receiver operating in the same frequency band.

This paper is organized as follows. Section II briefly reviews the system model introduced in Part I. Section III analyzes the channel capacity of the system, and presents numerical examples to illustrate its dependence on important network parameters. Section IV derives the power spectral density (PSD) of the aggregate interference, introduces the concept of spectral outage probability, and provides numerical examples of both metrics. Section V summarizes important findings.

II. Model Summary

We briefly review the model introduced in Part I. As shown in [8, Fig. 1], we consider the interfering nodes to be spatially scattered in the two-dimensional infinite plane, according to a homogeneous Poisson process with density λ (in nodes per unit area) [9]. The random distance of interfering node i to the origin is denoted by R_i. For analytical purposes, we introduce a *probe link* which is composed of two nodes: the *probe receiver* (located at the origin), and the *probe transmitter* (node $i = 0$).

In terms of transmission characteristics, we consider that all interfering nodes employ the same two-dimensional modulation and transmit at the same power P. For generality, however, we allow the probe transmitter to employ an arbitrary two-dimensional modulation and arbitrary power P_0, not

necessarily equal to that used by the interfering nodes. We consider that all nodes employ the same symbol rate $1/T$, but the signal received from node i is shifted by a random delay D_i, where $D_i \sim \mathcal{U}(0,T)$.[1] The probe receiver performs coherent demodulation of the desired signal using a conventional in-phase/quadrature (IQ) detector.

The wireless propagation channel introduces path loss, log-normal shadowing, and multipath fading. Specifically, the overall effect of the channel on node i is accounted for by the random phase $\phi_i \sim \mathcal{U}(0,2\pi)$, and the amplitude factor $\frac{k\alpha_i e^{\sigma G_i}}{R_i^b}$. The term $\frac{k}{R_i^b}$ accounts for the path loss; α_i is due to the multipath fading, and has an arbitrary distribution with $\mathbb{E}\{\alpha_i^2\}=1$; and $e^{\sigma G_i}$ is due to the log-normal shadowing, with $G_i \sim \mathcal{N}(0,1)$.[2]

In the rest of the paper, we consider the scenario where the location $\{R_i\}_{i=1}^{\infty}$ and shadowing $\{G_i\}_{i=1}^{\infty}$ of the interferers (succinctly denoted by $\mathcal{P}$), as well as the shadowing G_0 affecting the probe transmitter, remain approximately constant during the interval of interest. This models a quasi-static scenario where the movement of the nodes during the interval of interest is negligible. In such case, we condition the analysis on $\mathcal{P}$ in order to derive a *capacity outage probability* and a *spectral outage probability*, which are more meaningful than the corresponding $\mathcal{P}$-averaged metrics.[3] Other fast-varying propagation effects, such as multipath fading due to local scattering, are averaged out in the analysis.

III. Channel Capacity

In Part I of this paper, we focused on error performance metrics. We now build on the results of Part I and analyze the capacity of the link between the probe transmitter and probe receiver in [8, Fig. 1], subject to aggregate network interference and additive white Gaussian noise (AWGN). Unlike the simple AWGN channel, here the capacity depends on the information available about the channel at the probe transmitter and receiver. As in Part I, we assume that the probe receiver can perfectly estimate the fading (α_0 and ϕ_0) affecting its own link, thus ensuring that coherent demodulation of the desired signal is possible. The probe transmitter, on the other hand, is not able to estimate the channel. This corresponds to the scenario where the receiver has perfect knowledge of the channel state information (CSI).

A. Capacity Outage Probability

We start with the complex baseband characterization of the probe link, obtained in Part I by projecting all signals onto a cosine-sine orthonormal set. Thus, the complex channel output $\mathbf{Z}$ can be written as

$$\mathbf{Z} = \frac{\alpha_0 e^{\sigma G_0}}{r_0^b}\mathbf{S} + \widetilde{\mathbf{W}}, \tag{1}$$

where $\mathbf{S}$ is the complex channel input, and $\widetilde{\mathbf{W}}$ is the combined aggregate interference and thermal noise, given by

$$\widetilde{\mathbf{W}} = \sum_{i=1}^{\infty} \frac{e^{\sigma G_i}\mathbf{X}_i}{R_i^b} + \mathbf{W}, \tag{2}$$

with $\mathbf{W} \sim \mathcal{N}_{\mathrm{c}}(0,N_0)$.[4] These are essentially the same baseband equations as those given in Part I, except that the transmitted constellation symbol $a_0 e^{j\theta_0}$ has been replaced by a generic input symbol $\mathbf{S}$, with an arbitrary distribution $f_{\mathbf{S}}(\mathbf{s})$. This emphasizes the fact that to analyze the channel capacity, we need to maximize the mutual information over all possible input distributions $f_{\mathbf{S}}(\mathbf{s})$, and thus cannot restrict $\mathbf{S}$ to belong to a specific constellation, such as M-PSK or M-QAM. In addition, we impose an average energy constraint on the input symbol by requiring that $\mathbb{E}\{|\mathbf{S}|^2\} \le E_{\mathrm{S}}$.

Considering that the interfering nodes are coded and operating close to capacity, then the signal transmitted by each interferer is Gaussian, such that $\mathbf{X}_i \sim \mathcal{N}_{\mathrm{c}}(0,2V_X)$ [10].[5] The resulting aggregate interference is thus Gaussian when conditioned on $\mathcal{P}$, and the distribution of $\widetilde{\mathbf{W}}$ in (2) is given by[6]

$$\widetilde{\mathbf{W}} \overset{|\mathcal{P}}{\sim} \mathcal{N}_{\mathrm{c}}(0, 2AV_X + N_0), \tag{3}$$

where

$$A = \sum_{i=1}^{\infty} \frac{e^{2\sigma G_i}}{R_i^{2b}}. \tag{4}$$

Note that since A in (4) depends on $\mathcal{P}$ (i.e., $\{R_i\}_{i=1}^{\infty}$ and $\{G_i\}_{i=1}^{\infty}$), it can be seen as a random variable (r.v.) whose value is different for each realization of $\mathcal{P}$. It was shown in Part I that the r.v. A has a *skewed stable distribution* [11] given by[7]

$$A \sim \mathcal{S}\left(\alpha_A = \frac{1}{b},\ \beta_A = 1,\ \gamma_A = \lambda\pi\mathcal{C}_{1/b}^{-1} e^{2\sigma^2/b^2}\right), \tag{5}$$

where $b > 1$, and $\mathcal{C}_x$ is defined as

$$\mathcal{C}_x \triangleq \begin{cases} \frac{1-x}{\Gamma(2-x)\cos(\pi x/2)}, & x \neq 1, \\ \frac{2}{\pi}, & x = 1, \end{cases} \tag{6}$$

with $\Gamma(x) = \int_0^{\infty} t^{x-1}e^{-t}dt$ denoting the gamma function.

Because of the conditioning on G_0 and $\mathcal{P}$, equations (1)-(4) describe a simple Gaussian channel depicted schematically in Fig. 1. The capacity of this energy-constrained, fast fading channel with receiver CSI can be written as [12]

$$C = \max_{f_{\mathbf{S}}:\, \mathbb{E}|\mathbf{S}|^2 \le E_{\mathrm{S}}} I(\mathbf{S};\mathbf{Z}|\alpha_0),$$

[1] We use $\mathcal{U}(a,b)$ to denote a real uniform distribution in the interval $[a,b]$.

[2] We use $\mathbb{E}\{\cdot\}$ and $\mathbb{V}\{\cdot\}$ to denote the expectation and variance operators, respectively. In addition, we use $\mathcal{N}(\mu,\sigma^2)$ to denote a real Gaussian distribution with mean μ and variance σ^2.

[3] We implicitly assume conditioning on $\mathcal{P}$ in the rest of the paper, unless otherwise indicated.

[4] We use $\mathcal{N}_{\mathrm{c}}(0,\sigma^2)$ to denote a circularly symmetric (CS) complex Gaussian distribution, where the real and imaginary parts are independent identically distributed (i.i.d.) $\mathcal{N}(0,\sigma^2/2)$.

[5] Alternatively, we can follow the same approach as in Part I and argue that $\mathbf{X}_i \sim \mathcal{N}_{\mathrm{c}}(0,2V_X)$ in a scenario where the interferers employ an arbitrary two-dimensional modulation (this is the Gaussian approximation introduced in [8, Eq. (11)]). In such case, V_X is a function of the constellation of the interferers, as shown in [8, Eq. (14)].

[6] We use $X \overset{|Y}{\sim}$ to denote the distribution of X conditional on Y.

[7] We use $\mathcal{S}(\alpha,\beta,\gamma)$ to denote a real stable distribution with characteristic exponent $\alpha \in (0,2]$, skewness $\beta \in [-1,1]$, and dispersion $\gamma \in [0,\infty)$. The corresponding characteristic function is

$$\phi(w) = \begin{cases} \exp\left[-\gamma|w|^{\alpha}\left(1 - j\beta\,\mathrm{sign}(w)\tan\frac{\pi\alpha}{2}\right)\right], & \alpha \neq 1, \\ \exp\left[-\gamma|w|\left(1 + j\frac{2}{\pi}\beta\,\mathrm{sign}(w)\ln|w|\right)\right], & \alpha = 1. \end{cases}$$

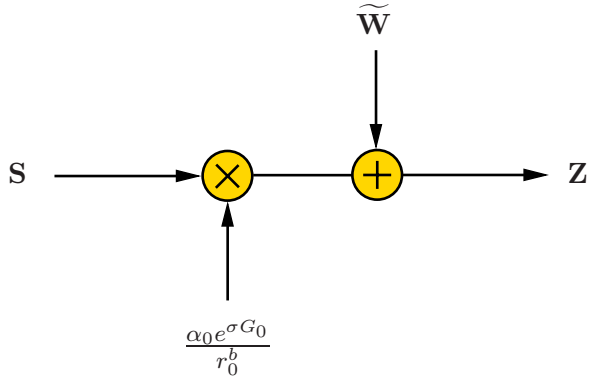

Fig. 1. Channel model for capacity analysis.

where $I(\mathbf{S};\mathbf{Z}|\alpha_0)$ is the conditional mutual information between $\mathbf{S}$ and $\mathbf{Z}$ given α_0. The optimal input distribution that maximizes the mutual information is therefore $\mathcal{N}_c(0, E_S)$. With this input distribution,

$$I(\mathbf{S};\mathbf{Z}|\alpha_0 = \widetilde{\alpha}_0) = \log_2\left(1 + \frac{\widetilde{\alpha}_0^2 e^{2\sigma G_0} E_S}{r_0^{2b}(2AV_X + N_0)}\right)$$

in bits per complex symbol, and thus we obtain the capacity of the channel as

$$C(G_0, \mathcal{P}) = \mathbb{E}_{\alpha_0}\left\{\log_2\left(1 + \frac{\alpha_0^2 e^{2\sigma G_0} E_S}{r_0^{2b}(2AV_X + N_0)}\right)\middle| G_0, A\right\} \tag{7}$$

in bits per complex symbol, where we have explicitly indicated the conditioning of C on the random interferer positions and shadowing. For a Rayleigh fading channel, α_0^2 is exponentially distributed with mean 1 and we can further express (7) in terms of the exponential integral function $\mathrm{Ei}(x) = -\int_{-x}^{\infty} \frac{e^{-t}}{t} dt$ as

$$C(G_0, \mathcal{P}) = -\frac{\exp\left(\frac{\sqrt{2}}{\eta}\right)}{\ln(2)} \mathrm{Ei}\left(-\frac{\sqrt{2}}{\eta}\right) \tag{8}$$

in bits per complex symbol, where

$$\eta = \frac{e^{2\sigma G_0} E_S}{r_0^{2b}(2AV_X + N_0)} \tag{9}$$

is the received signal-to-interference-plus-noise ratio (SINR), averaged over the fast fading.

In the proposed quasi-static model, the maximum rate of reliable communication for a given realization of G_0 and $\mathcal{P}$ is given by (8)-(9). Such quantity is a function of the random user positions and shadowing, and is therefore random. Then, with some probability, G_0 and $\mathcal{P}$ are such that the capacity is below the desired transmission rate ϱ, thus making the channel unusable for communication at that rate with arbitrarily low error probability. The system is said to be *in outage*, and the capacity outage probability is

$$P_{\text{out}}^{\text{c}} = \mathbb{P}_{G_0,\mathcal{P}}\{C(G_0, \mathcal{P}) < \varrho\}, \tag{10}$$

or, substituting (8) into (10),

$$P_{\text{out}}^{\text{c}} = \mathbb{P}_{\eta}\left\{-\frac{\exp\left(\frac{\sqrt{2}}{\eta}\right)}{\ln(2)} \mathrm{Ei}\left(-\frac{\sqrt{2}}{\eta}\right) < \varrho\right\}. \tag{11}$$

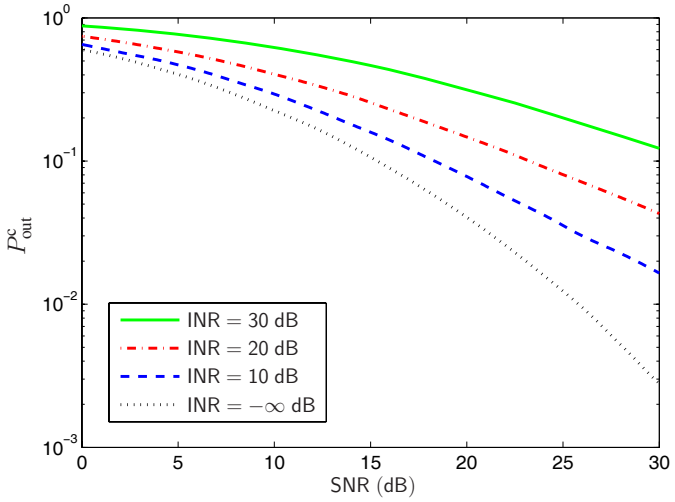

Fig. 2. Capacity outage probability $P_{\text{out}}^{\text{c}}$ versus the SNR of the probe link, for various interferer-to-noise ratios INR ($\varrho = 1$ bit/complex symbol, $\lambda = 0.01\,\text{m}^{-2}$, $b = 2$, $r_0 = 1\,\text{m}$, $\sigma_{\text{dB}} = 10$).

B. Numerical Results

Figures 2 and 3 quantify the capacity outage probability and illustrate its dependence on the various parameters, such as the signal-to-noise ratio $\mathsf{SNR} = E_S/N_0$, the interference-to-noise ratio $\mathsf{INR} = E/N_0$, and spatial density λ of the interferers. For simplicity, we consider a case study where all interfering nodes transmit equiprobable symbols, belonging to a constellation that is symmetric with respect to the origin of the IQ-plane (e.g., M-PSK and M-QAM). In this particular case, it is shown in [8, Eq. (14)] that $V_X = E/3$, and thus (9) reduces to

$$\eta = \frac{e^{2\sigma G_0}\mathsf{SNR}}{r_0^{2b}\left(\frac{2A}{3}\mathsf{INR} + 1\right)}. \tag{12}$$

To evaluate the corresponding $P_{\text{out}}^{\text{c}}$, we resort to a hybrid approach where we employ the analytical result given in (11)-(12), but perform a Monte Carlo simulation of the stable r.v. A according to [13]. Nevertheless, we emphasize that the expressions derived in this paper completely eliminate the need for simulation of the interferers' positions and waveforms in the network, in order to obtain the capacity.

IV. Spectral Characterization of the Aggregate Network Emission

The spectral properties of the aggregate RF emission generated by all the nodes in a network is an important consideration in the design of wireless systems. This is useful in military applications, for example, where the communication designer must ensure that the presence of the deployed network is not detected by the enemy. If, for example, a sensor network is to be deployed in enemy territory, then the characterization of the aggregate network emission is essential for the design of a covert system. In commercial applications, on the other hand, the goal is to ensure that the RF emission of the network does not cause interference to other systems operating in overlapping frequency bands. To prevent interference, many commercial networks operate under restrictions which often take the form of spectral masks, imposed by a regulatory

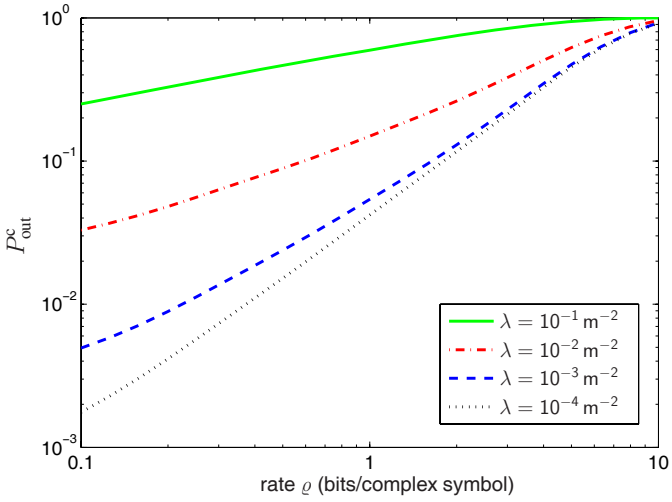

Fig. 3. Capacity outage probability $P_{\text{out}}^{\text{c}}$ versus the desired transmission rate ϱ, for various interferer spatial densities λ (SNR = INR = 20 dB, $b = 2$, $r_0 = 1\,\text{m}$, $\sigma_{\text{dB}} = 10$).

agency such as the US Federal Communications Commission (FCC).

In the previous sections, we have so far derived the error probability and capacity of a link subject to both network interference and thermal noise. We now determine the PSD of the aggregate interference process $\mathbf{Y}(t)$, measured at the origin of the two-dimensional plane in [8, Fig. 1]. The spectral characteristics of $\mathbf{Y}(t)$ can be inferred from the knowledge of its PSD.

A. Power Spectral Density of the Aggregate Network Emission

The aggregate network emission at the probe receiver can be characterized by the complex baseband random process $\mathbf{Y}(t)$, defined as

$$\mathbf{Y}(t) = \sum_{i=1}^{\infty} \mathbf{Y}_i(t), \tag{13}$$

where $\mathbf{Y}_i(t)$ is the received process associated with each emitting node i. The signal $\mathbf{Y}_i(t)$ can in turn be expressed for all time t as

$$\mathbf{Y}_i(t) = \frac{e^{\sigma G_i}}{R_i^b} \int \mathbf{h}_i(t,\tau)\mathbf{X}_i(t-\tau)d\tau, \tag{14}$$

where $\mathbf{X}_i(t)$ is the complex baseband transmitted signal, and $\mathbf{h}_i(t,\tau)$ is time-varying complex baseband impulse response of the multipath channel associated with node i. The system model described by (14) is depicted in Fig. 4. It corresponds to a generalization of the model introduced in Part I of this paper, where we considered a two-dimensional modulation and a flat Rayleigh fading channel. Since now we are interested in analyzing the spectral properties of $\mathbf{Y}(t)$, we incorporate in the model a generic transmitted waveform $\mathbf{X}_i(t)$, not necessarily associated with a two-dimensional modulation, as well as a generic multipath channel $\mathbf{h}_i(t,\tau)$, not necessarily associated with flat Rayleigh fading. Also, since in this section we are only interested in the aggregate emission of the network, we can ignore the existence of the probe link depicted in [8, Fig. 1]. In the remainder of this paper, we carry the analysis

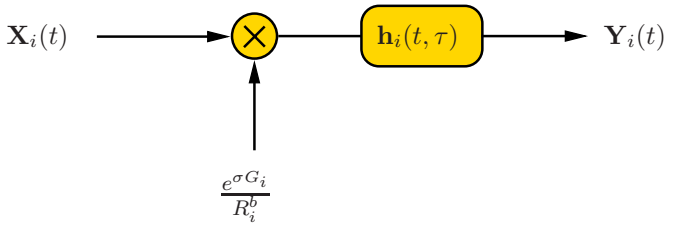

Fig. 4. Channel model for spectral analysis.

in complex baseband, although it can be trivially translated to passband frequencies.

In what follows, we consider that the transmitted signal $\mathbf{X}_i(t)$ is a *wide-sense stationary* (WSS) process, such that its autocorrelation function has the form $R_{\mathbf{X}_i}(t_1,t_2) \triangleq \mathbb{E}\{\mathbf{X}_i^*(t_1)\mathbf{X}_i(t_2)\} = R_{\mathbf{X}}(\Delta t)$, where $\Delta t = t_2 - t_1$. We define the PSD of the process $\mathbf{X}_i(t)$ as $\mathcal{S}_{\mathbf{X}}(f) \triangleq \mathcal{F}_{\Delta t \to f}\{R_{\mathbf{X}}(\Delta t)\}$.[8] Since different nodes operate independently, the processes $\mathbf{X}_i(t)$ are also independent for different i, but the underlying second-order statistics are the same (i.e., the autocorrelation function and the PSD of $\mathbf{X}_i(t)$ do not depend on i). As we will show in the case study of Section IV-C, if $\mathbf{X}_i(t)$ is a train of pulses with a uniformly distributed random delay (which models the asynchronism between emitting nodes), then it is a WSS process.

To model the multipath effect, we consider a *wide-sense stationary uncorrelated scattering* (WSSUS) channel [14]–[18], so that the autocorrelation function of $\mathbf{h}_i(t,\tau)$ can be expressed as

$$\begin{aligned} R_{\mathbf{h}_i}(t_1,t_2,\tau_1,\tau_2) &\triangleq \mathbb{E}\{\mathbf{h}_i^*(t_1,\tau_1)\mathbf{h}_i(t_2,\tau_2)\} \\ &= P_{\mathbf{h}}(\Delta t,\tau_2)\delta(\tau_2-\tau_1), \end{aligned}$$

for some function $P_{\mathbf{h}}(\Delta t,\tau)$. Such channel can be represented in the form of a densely-tapped delay line, as a continuum of uncorrelated, randomly-scintillating scatterers having WSS statistics. The functions $\mathbf{h}_i(t,\tau)$ are considered to be independent for different nodes i, but the underlying second-order statistics are the same (i.e., the autocorrelation function of $\mathbf{h}_i(t,\tau)$ does not depend on i). WSSUS channels are an important class of practical channels which simultaneously exhibit wide-sense stationarity in the time variable t and uncorrelated scattering in the delay variable τ. They are the simplest non-degenerate channels which exhibit both time and frequency fading, and also serve as a good model for many radio channels.

We are now interested in determining the PSD of the aggregate RF emission $\mathbf{Y}(t)$ of the network. The result is given in the following theorem.

Theorem 4.1 (WSS and WSSUS Channels): Let $\mathbf{h}(t,\tau)$ denote the time-varying complex baseband impulse response of a multipath channel, whose autocorrelation function is given by $R_{\mathbf{h}}(t_1,t_2,\tau_1,\tau_2)$. Let $\mathbf{u}(t)$ denote the complex baseband WSS process which is applied as input to the channel, and $\mathbf{z}(t)$ denote the corresponding output process of the channel.

1) If the channel $\mathbf{h}(t,\tau)$ is WSS, i.e., $R_{\mathbf{h}}(t_1,t_2,\tau_1,\tau_2) = R_{\mathbf{h}}(\Delta t,\tau_1,\tau_2)$, then the output $\mathbf{z}(t)$ is WSS and its PSD

[8]We use $\mathcal{F}_{x\to y}\{\cdot\}$ to denote the Fourier transform operator, where x and y represent the independent variables in the original and transformed domains, respectively.

is given by[9]

$$\mathcal{S}_{\mathbf{z}}(f) = \iint P_{\mathrm{s}}(\nu, \tau_1, \tau_2)|_{\nu=f} \overset{f}{*} \left[\mathcal{S}_{\mathbf{u}}(f) e^{j2\pi f(\tau_1-\tau_2)}\right] d\tau_1 d\tau_2, \tag{15}$$

where $P_{\mathrm{s}}(\nu, \tau_1, \tau_2) \triangleq \mathcal{F}_{\Delta t \to \nu}\{R_{\mathbf{h}}(\Delta t, \tau_1, \tau_2)\}$, and $\mathcal{S}_{\mathbf{u}}(f)$ is the PSD of $\mathbf{u}(t)$.

2) If the channel $\mathbf{h}(t, \tau)$ is WSSUS, i.e., $R_{\mathbf{h}}(t_1, t_2, \tau_1, \tau_2) = P_{\mathbf{h}}(\Delta t, \tau_2)\delta(\tau_2 - \tau_1)$ for some function $P_{\mathbf{h}}(\Delta t, \tau)$, then the output $\mathbf{z}(t)$ is WSS and its PSD is given by

$$\mathcal{S}_{\mathbf{z}}(f) = \mathcal{D}_{\mathbf{h}}(\nu)|_{\nu=f} \overset{f}{*} \mathcal{S}_{\mathbf{u}}(f), \tag{16}$$

where $\mathcal{D}_{\mathbf{h}}(\nu) \triangleq \int P_{\mathrm{s}}(\nu, \tau) d\tau$ is the *Doppler power spectrum* of the channel $\mathbf{h}(t, \tau)$, and $P_{\mathrm{s}}(\nu, \tau) \triangleq \mathcal{F}_{\Delta t \to \nu}\{P_{\mathbf{h}}(\Delta t, \tau)\}$ is the *scattering function* of the channel $\mathbf{h}(t, \tau)$.

Proof: See Appendix A for a proof and an intuitive interpretation of the theorem. □

The theorem implies that the signal $\mathbf{Y}_i(t)$ in (14) is WSS and thus the aggregate network emission $\mathbf{Y}(t)$ is also WSS. Furthermore, the PSD of $\mathbf{Y}_i(t)$ is given by

$$\mathcal{S}_{\mathbf{Y}_i}(f) = \frac{e^{2\sigma G_i}}{R_i^{2b}} \left[\mathcal{D}_{\mathbf{h}}(f) * \mathcal{S}_{\mathbf{X}}(f)\right], \tag{17}$$

where $\mathcal{D}_{\mathbf{h}}(f)$ is the Doppler power spectrum of the time-varying multipath channel $\mathbf{h}_i(t, \tau)$, and $\mathcal{S}_{\mathbf{X}}(f)$ is the PSD of the transmitted signal $\mathbf{X}_i(t)$. Because the processes $\mathbf{Y}_i(t)$ associated with different emitting nodes i are statistically independent when conditioned on $\mathcal{P}$, we can write

$$\mathcal{S}_{\mathbf{Y}}(f) = \sum_{i=1}^{\infty} \mathcal{S}_{\mathbf{Y}_i}(f). \tag{18}$$

Combining (17) and (18), we obtain the desired conditional PSD of the aggregate network emission $\mathbf{Y}(t)$ as

$$\mathcal{S}_{\mathbf{Y}}(f, \mathcal{P}) = A \left[\mathcal{D}_{\mathbf{h}}(f) * \mathcal{S}_{\mathbf{X}}(f)\right], \tag{19}$$

where A was defined in (4). Note that in (19) we explicitly indicated the conditioning of $\mathcal{S}_{\mathbf{Y}}$ on the random node positions and shadowing, $\mathcal{P}$. Since $\mathcal{S}_{\mathbf{Y}}(f, \mathcal{P})$ depends on $\mathcal{P}$, it can be viewed, for a fixed f, as a r.v. whose value is different for each realization of $\mathcal{P}$.[10] Finally, we recall that A, when seen as a r.v., has the skewed stable distribution given in (5).

B. Spectral Outage Probability

In the previous section, we derived the PSD of the aggregate network emission, $\mathcal{S}_{\mathbf{Y}}(f, \mathcal{P})$, and showed that it is a function of the random node positions and shadowing, $\mathcal{P}$. Then, with some probability, $\mathcal{P}$ is such that the spectrum of the aggregate emission is too high in some frequency band of interest, thus causing an outage in that frequency band. This leads to the concept of *spectral outage probability* (SOP), which we denote by $P_{\mathrm{out}}^{\mathrm{s}}(f)$ and generally define as

$$P_{\mathrm{out}}^{\mathrm{s}}(f) \triangleq \mathbb{P}_{\mathcal{P}}\{\mathcal{S}_{\mathbf{Y}}(f, \mathcal{P}) > m(f)\}, \tag{20}$$

where $\mathcal{S}_{\mathbf{Y}}(f, \mathcal{P})$ is the random PSD of the aggregate network emission $\mathbf{Y}(t)$, and $m(f)$ is some spectral mask determining the outage (or detection) threshold at the receiver. The SOP is a frequency-dependent quantity and, in the case of slow-varying positions $\mathcal{P}$, is a more insightful metric than the PSD averaged over $\mathcal{P}$. Note that this definition is applicable in general to any emission model: the spectral outage probability $P_{\mathrm{out}}^{\mathrm{s}}(f)$ represents the probability that the PSD of the aggregate network emission, measured at an arbitrary location in the plane and at a particular frequency f, exceeds some predetermined mask [19].

In commercial applications, the concept of SOP can provide a radically different way to establish spectral regulations. Current regulations and standards (e.g., FCC Part 15 or IEEE 802.11) impose a spectral mask on the PSD *at the transmitter*, and the type of mask often depends on the environment in which the devices are operated (e.g., indoor or outdoor). The purpose of this mask is to limit RF emissions generated by a terminal, and to protect other services that operate in dedicated bands (e.g., Global Positioning System, public safety, and cellular systems). However, the *transmitted* PSD is usually not representative of the aggregate PSD *at the victim receiver*, due to the random propagation effects (multipath fading and shadowing) and the random position of the emitting nodes. Thus, spectral regulations that are based only on the transmitted PSD do not necessarily protect a victim receiver against interference.

In the proposed framework, we follow a radically different approach, in the sense that the spectral mask is defined at the victim receiver, not at the transmitter. In effect, the mask $m(f)$ introduced in (20) represents the outage threshold with respect to the *accumulated PSD at the receiver*, not the individual PSD at the transmitter (this follows from the fact that $\mathcal{S}_{\mathbf{Y}}(f, \mathcal{P})$ is measured at an arbitrary location in the plane, where a probe receiver could be located). Therefore, the received aggregate spectrum $\mathcal{S}_{\mathbf{Y}}(f, \mathcal{P})$ and the corresponding $P_{\mathrm{out}}^{\mathrm{s}}(f)$ can be used to characterize and control the network's RF emissions more effectively, since they not only consider the aggregate effect of all emitting nodes at an arbitrary receiver location, but also incorporate the random propagation effects and random node positions. Furthermore, the use of different masks for indoor or outdoor environments is no longer necessary, since the environment is already accounted for in our model by parameters such as the amplitude loss exponent b, the spatial density λ of the emitting nodes, and the shadowing coefficient σ.

In military applications, on the other hand, the goal is to ensure that the presence of the deployed network is not detected by the enemy. If, for example, a surveillance network is to be deployed in enemy territory, then the characterization of its aggregate emission is essential for the design of a covert network with low probability of detection. In such application, the function $m(f)$ in (20) can be interpreted as the frequency-dependent mask which determines the *detection threshold* (not the outage threshold as before). In other words, if the aggregate spectral density $\mathcal{S}_{\mathbf{Y}}(f, \mathcal{P})$ measured at a given location exceeds the mask $m(f)$, then the presence of the deployed network could be detected by the enemy.

For the signal model considered in this paper, $P_{\mathrm{out}}^{\mathrm{s}}(f)$ can be derived by substituting (19) into the general definition of

[9] We use $\overset{x}{*}$ to denote the convolution operation with respect to variable x.

[10] $\mathcal{S}_{\mathbf{Y}}(f, \mathcal{P})$ is in fact a random process whose sample paths evolve in *frequency* instead of *time*. For each realization $\mathcal{P} = \mathcal{P}_0$, we obtain a sample path $\mathcal{S}_{\mathbf{Y}}(f, \mathcal{P}_0)$ that is a function of f; for a fixed frequency $f = f_0$, $\mathcal{S}_{\mathbf{Y}}(f_0, \mathcal{P})$ is a r.v.

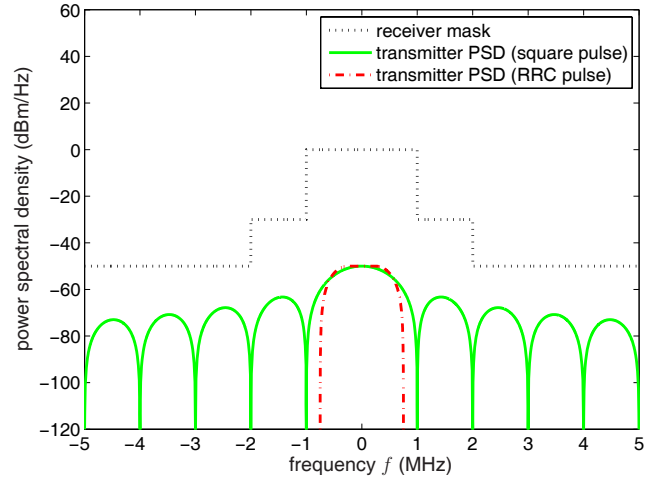

(a) PSD of the individual transmitted signal versus frequency (bottom curves), for various pulse shapes $g(t)$. The square and RRC pulses are normalized so that the transmitted signals have the same power P. The piecewise-constant spectral mask $m(f)$ (top curve) determines the outage threshold at the receiver.

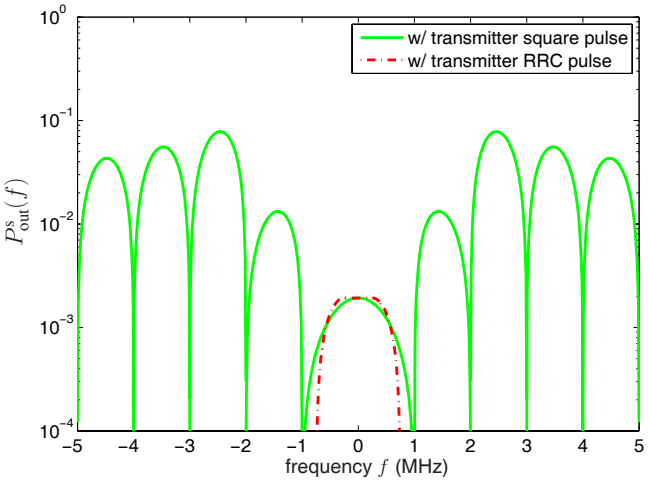

(b) Spectral outage probability $P^{\mathrm{s}}_{\mathrm{out}}(f)$ versus frequency, for the piecewise-constant mask $m(f)$ shown in (a).

Fig. 5. Effect of the transmitted baseband pulse shape $g(t)$ on the PSD and the outage probability $P^{\mathrm{s}}_{\mathrm{out}}(f)$ ($P = 10\,\mathrm{dBm}$, $T = 10^{-6}\,\mathrm{s}$, $\lambda = 0.1\,\mathrm{m}^{-2}$, $b = 2$, $\sigma_{\mathrm{dB}} = 10$, RRC pulse with rolloff factor 0.5).

SOP in (20), leading to

$$P^{\mathrm{s}}_{\mathrm{out}}(f) = \mathbb{P}\left\{A > \frac{m(f)}{\mathcal{D}_{\mathbf{h}}(f) * \mathcal{S}_{\mathbf{X}}(f)}\right\} = 1 - F_A\left(\frac{m(f)}{\mathcal{D}_{\mathbf{h}}(f) * \mathcal{S}_{\mathbf{X}}(f)}\right), \tag{21}$$

where $F_A(\cdot)$ is the cumulative distribution function (c.d.f.) of the stable r.v. A, whose distribution is given in (5).

C. Numerical Results

In this section, we quantify the spectral density and outage probability associated with a particular case study. We also illustrate their dependence on the various parameters involved, such as the transmitted pulse shape, spectral mask, transmitted power, and spatial density of the emitting nodes. For all numerical examples, we consider that the emitting nodes employ a two-dimensional modulation (e.g., M-PSK or M-QAM), such that transmitted signal $\mathbf{X}_i(t)$ can be written for all t as

$$\mathbf{X}_i(t) = \sum_{n=-\infty}^{+\infty} \mathbf{a}_{i,n} g(t - nT - D_i), \tag{22}$$

where the sequence $\{\mathbf{a}_{i,n}\}_{n=-\infty}^{+\infty}$ represents the stream of complex symbols transmitted by node i, assumed to be i.i.d. in n and zero-mean, for simplicity; $g(t)$ is a real, baseband, unit-energy shaping pulse, defined for all values of t; T is the symbol period; and $D_i \sim \mathcal{U}(0,T)$ is a random delay representing the asynchronism between different emitting nodes. The type of constellation employed by the emitting nodes is captured by the statistics of the symbols $\{\mathbf{a}_{i,n}\}$.[11] Note that the process $\mathbf{X}_i(t)$ in (22) is WSS, as required by Theorem 4.1.[12] The PSD of $\mathbf{X}_i(t)$ is then given by [21]–[23]

$$\mathcal{S}_{\mathbf{X}}(f) = P|G(f)|^2, \tag{23}$$

where $P = \mathbb{E}\{|\mathbf{a}_{i,n}|^2\}/T$ is the power transmitted by each emitting node, and $G(f) = \mathcal{F}\{g(t)\}$.

To model the multipath effect, we consider for simplicity that $\mathbf{h}(t,\tau)$ is time-invariant such that it does not introduce any Doppler shifts, i.e., $\mathcal{D}_{\mathbf{h}}(\nu) = \delta(\nu)$.[13] Substituting the expressions for $\mathcal{S}_{\mathbf{X}}(f)$ and $\mathcal{D}_{\mathbf{h}}(\nu)$ in (21), we obtain the SOP as

$$P^{\mathrm{s}}_{\mathrm{out}}(f) = 1 - F_A\left(\frac{m(f)}{P|G(f)|^2}\right). \tag{24}$$

Figure 5 shows that for a fixed spectral mask $m(f)$, the SOP can be highly dependent on the pulse shape $g(t)$, such as square or root raised-cosine (RRC) pulse. In fact, $P^{\mathrm{s}}_{\mathrm{out}}(f)$ is a nonlinear function of $|G(f)|$, where the nonlinearity is determined in part by the c.d.f. $F_A(\cdot)$ of the stable r.v. A, as shown in (24). The SOP can be used as a criterion for designing the pulse shape: for example, we may wish to determine the baseband pulse $g(t)$ and transmitted power P such that $\max_f P^{\mathrm{s}}_{\mathrm{out}}(f) \leq p^*$, where p^* is some target outage probability which must be satisfied at all frequencies.

Figure 6 shows that for a fixed pulse shape $g(t)$, $P^{\mathrm{s}}_{\mathrm{out}}(f)$ can significantly depend on the spectral mask $m(f)$ (e.g., piecewise-linear, Gaussian, or constant mask). Since $P^{\mathrm{s}}_{\mathrm{out}}(f)$ accounts for both $G(f)$ and $m(f)$, it quantifies the compatibility of the transmitted pulse shape with the spectral restrictions imposed through $m(f)$.

Figures 7 and 8 illustrate, respectively, the dependence of the outage probability $P^{\mathrm{s}}_{\mathrm{out}}(f)$ on the transmitted power P and spatial density λ of the emitting nodes. Specifically, as P or λ increase, the aggregate network emission becomes stronger, and thus $P^{\mathrm{s}}_{\mathrm{out}}(f)$ deteriorates at all frequencies, approaching the maximum value of 1.

[11]Note that each complex symbol $\mathbf{a}_{i,n} = a_{i,n}e^{j\theta_{i,n}}$ can be represented in the IQ plane by a constellation point with amplitude $a_{i,n}$ and phase $\theta_{i,n}$.

[12]This can be shown in the following way: first, if we deterministically set D_i to zero in (22), the resulting process $\tilde{\mathbf{X}}_i(t)$ is wide-sense cyclostationary (WSCS) with period T [20]; then, since $\mathbf{X}_i(t) = \tilde{\mathbf{X}}_i(t - D_i)$, with $D_i \sim \mathcal{U}(0,T)$ and independent of everything else, it follows that $\mathbf{X}_i(t)$ is WSS.

[13]For typical node speeds or channel fluctuations, the frequencies of the Doppler shifts are on the order of few KHz. As a consequence, when the considered $\mathbf{X}_i(t)$ is an ultrawideband signal, $\mathcal{D}_{\mathbf{h}}(\nu)$ can be well approximated by a Dirac-delta function.

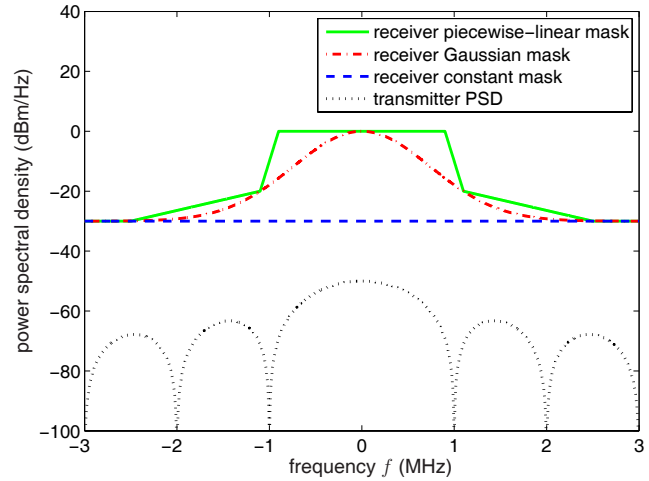

(a) Plot of various spectral masks $m(f)$ which define the outage threshold at the receiver (top curves). Also shown is the PSD of the individual transmitted signal versus frequency (bottom curve).

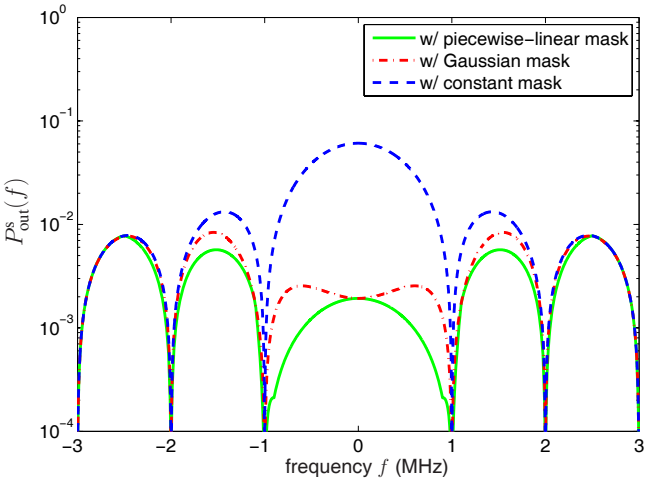

(b) Spectral outage probability $P^{\mathrm{s}}_{\mathrm{out}}(f)$ versus frequency, for the various masks $m(f)$ shown in (a).

Fig. 6. Effect of the spectral mask shape $m(f)$ on the outage probability $P^{\mathrm{s}}_{\mathrm{out}}(f)$ (square $g(t)$, $P = 10\,\mathrm{dBm}$, $T = 10^{-6}$ s, $\lambda = 0.1\,\mathrm{m}^{-2}$, $b = 2$, $\sigma_{\mathrm{dB}} = 10$).

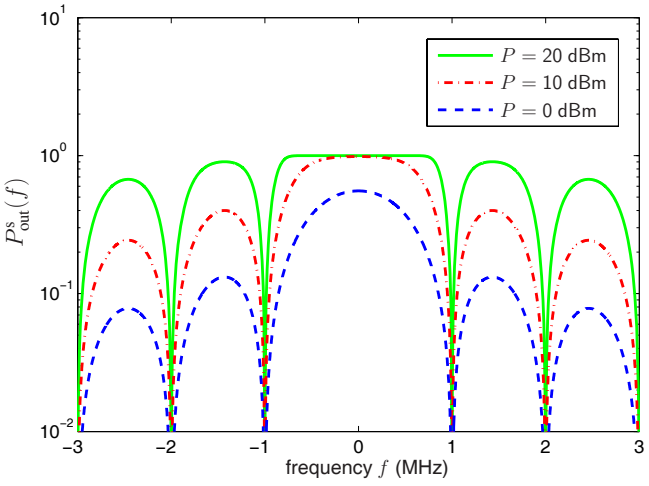

Fig. 7. Spectral outage probability $P^{\mathrm{s}}_{\mathrm{out}}(f)$ versus frequency, for various transmitted powers P (square $g(t)$, $T = 10^{-6}$ s, $\lambda = 0.1\,\mathrm{m}^{-2}$, $b = 2$, $\sigma_{\mathrm{dB}} = 10$, $m(f) = -60\,\mathrm{dBm/Hz}$).

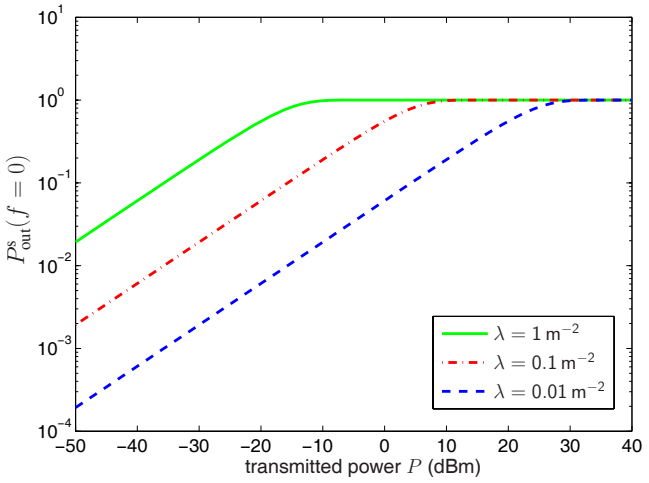

Fig. 8. Spectral outage probability $P^{\mathrm{s}}_{\mathrm{out}}(f)$, evaluated at $f = 0$, versus transmitted power P, for various spatial densities λ of the emitting nodes (square $g(t)$, $T = 10^{-6}$ s, $b = 2$, $\sigma_{\mathrm{dB}} = 10$, $m(f) = -60\,\mathrm{dBm/Hz}$).

D. Generalizations

We now extend the results to an heterogeneous scenario with K different networks, where a given emitting node belongs to the network $k \in \{1 \dots K\}$ with probability p_k, independently of everything else. Using the splitting property of Poisson processes [24], we know the emitting nodes from each network k form a spatial Poisson process, which is independent of the processes of other networks and has spatial density $\lambda_k = \lambda p_k$. Therefore, we can write the aggregate emission from all nodes in all networks as

$$\mathbf{Y}(t) = \sum_{k=1}^{K} \mathbf{Y}^{(k)}(t),$$

where $\mathbf{Y}^{(k)}(t) = \sum_{i=1}^{\infty} \mathbf{Y}_{k,i}(t)$ is the aggregate emission from the individual network k, and

$$\mathbf{Y}_{k,i}(t) = \frac{e^{\sigma G_{k,i}}}{R_{k,i}^{b}} \int \mathbf{h}_{k,i}(t,\tau)\mathbf{X}_{k,i}(t-\tau)d\tau, \quad k = 1 \dots K,$$

where $\mathbf{X}_{k,i}(t)$ and $\mathbf{h}_{k,i}(t,\tau)$ are, respectively, the transmitted signal and the impulse response of the multipath channel associated with node i from network k. We consider that $\mathbf{X}_{k,i}(t)$ and $\mathbf{h}_{k,i}(t,\tau)$ are independent in both k and i. Then, the aggregate emission $\mathbf{Y}^{(k)}(t)$ is also independent for different networks k when conditioned on the positions $\mathcal{P}$, and thus $\mathcal{S}_{\mathbf{Y}}(f) = \sum_{k=1}^{K} \mathcal{S}_{\mathbf{Y}^{(k)}}(f)$. We can generalize (19) and write the conditional PSD of the aggregate emission $\mathbf{Y}(t)$ in this heterogeneous scenario as

$$\mathcal{S}_{\mathbf{Y}}(f,\mathcal{P}) = \sum_{k=1}^{K} A_k \left[\mathcal{D}_{\mathbf{h}_k}(f) * \mathcal{S}_{\mathbf{X}_k}(f)\right],$$

where $\mathcal{D}_{\mathbf{h}_k}(f)$ and $\mathcal{S}_{\mathbf{X}_k}(f)$ are, respectively, the Doppler power spectrum and the PSD of the transmitted signal associated with network k; and the r.v.'s $\{A_k\}$ are i.i.d. in k and given by

$$A_k = \sum_{i=1}^{\infty} \frac{e^{2\sigma G_{k,i}}}{R_{k,i}^{2b}},$$

with distribution

$$A_k \sim \mathcal{S}\left(\alpha_A = \frac{1}{b},\ \beta_A = 1,\ \gamma_A = \pi\lambda_k \mathcal{C}_{1/b}^{-1} e^{2\sigma^2/b^2}\right).$$

V. Conclusions

This two-part paper investigates a mathematical model for communication subject to both network interference and AWGN, where the spatial distribution of the nodes is captured by a Poisson field in the two-dimensional plane. We specifically address the cases of slow and fast-varying node positions, as well as homogeneous and heterogeneous networks, in a realistic wireless environment subject to path loss, multipath fading and shadowing. In Part I, we determined the statistical distribution of the aggregate interference at the output of a conventional linear receiver, which leads directly to the characterization of the error performance (in terms of outage and average probabilities).

In this second part, we characterized the capacity of the link when subject to both network interference and noise, and derived the PSD of the aggregate RF emission of the network. Then, we put forth the concept of spectral outage probability, and described some possible applications, namely the establishment of spectral regulations and the design of covert military networks. In particular, the SOP can be used as a criterion for designing pulse shapes or controlling interference in wireless networks, and as a measure of the network's covertness. Our framework clearly shows how the aggregate network emission can be characterized in terms of important network parameters, thereby providing insights that may be of value to the network designer.

Appendix A
Derivation of Theorem 4.1

The derivation of Theorem 4.1 relies on the general theory of linear time-varying systems and Bello system functions [14]–[17]. Let $\mathbf{h}(t,\tau)$ denote a time-varying complex baseband impulse response of a multipath channel. When the complex baseband process $\mathbf{u}(t)$ is applied as input to the channel, the output process $\mathbf{z}(t)$ is given by the integral

$$\mathbf{z}(t) = \int \mathbf{h}(t,\tau)\mathbf{u}(t-\tau)d\tau.$$

We define the autocorrelation function of the input $\mathbf{u}(t)$ as $R_{\mathbf{u}}(t_1,t_2) \triangleq \mathbb{E}\{\mathbf{u}^*(t_1)\mathbf{u}(t_2)\}$, and the autocorrelation function of the channel $\mathbf{h}(t,\tau)$ as $R_{\mathbf{h}}(t_1,t_2,\tau_1,\tau_2) \triangleq \mathbb{E}\{\mathbf{h}^*(t_1,\tau_1)\mathbf{h}(t_2,\tau_2)\}$. The autocorrelation of the output $\mathbf{z}(t)$ is generally given by

$$R_{\mathbf{z}}(t_1,t_2) = \iint R_{\mathbf{h}}(t_1,t_2,\tau_1,\tau_2)R_{\mathbf{u}}(t_1-\tau_1,t_2-\tau_2)d\tau_1 d\tau_2. \tag{25}$$

Since the input process $\mathbf{u}(t)$ is WSS, $R_{\mathbf{u}}(t_1,t_2) = R_{\mathbf{u}}(\Delta t)$, where $\Delta t = t_2 - t_1$.

We first consider a WSS channel $\mathbf{h}(t,\tau)$ such that $R_{\mathbf{h}}(t_1,t_2,\tau_1,\tau_2) = R_{\mathbf{h}}(\Delta t,\tau_1,\tau_2)$. Then, we can rewrite $R_{\mathbf{z}}(t_1,t_2)$ in (25) as

$$\begin{aligned} R_{\mathbf{z}}(t_1,t_2) &= \iint R_{\mathbf{h}}(\Delta t,\tau_1,\tau_2)R_{\mathbf{u}}(\Delta t+\tau_1-\tau_2)d\tau_1 d\tau_2 \\ &\triangleq R_{\mathbf{z}}(\Delta t). \end{aligned} \tag{26}$$

Since $R_{\mathbf{z}}(t_1,t_2)$ is a function only of Δt, the output $\mathbf{z}(t)$ is also WSS. The PSD of $\mathbf{z}(t)$ can be written as

$$\begin{aligned} \mathcal{S}_{\mathbf{z}}(f) &= \mathcal{F}_{\Delta t\to f}\{R_{\mathbf{z}}(\Delta t)\} \\ &= \iint\left[\int R_{\mathbf{h}}(\Delta t,\tau_1,\tau_2)R_{\mathbf{u}}(\Delta t+\tau_1-\tau_2)\right. \\ &\qquad \left.\times e^{-j2\pi f\cdot\Delta t}d(\Delta t)\right]d\tau_1 d\tau_2 \\ &= \iint P_{\mathrm{s}}(\nu,\tau_1,\tau_2)|_{\nu=f} \overset{f}{*} \left[\mathcal{S}_{\mathbf{u}}(f)e^{j2\pi f(\tau_1-\tau_2)}\right]d\tau_1 d\tau_2, \end{aligned} \tag{27}$$

where $P_{\mathrm{s}}(\nu,\tau_1,\tau_2) \triangleq \mathcal{F}_{\Delta t\to\nu}\{R_{\mathbf{h}}(\Delta t,\tau_1,\tau_2)\}$, and $\mathcal{S}_{\mathbf{u}}(f)$ is the PSD of $\mathbf{u}(t)$. This is the result in Theorem 4.1, eq. (15).

We now further constrain the channel $\mathbf{h}(t,\tau)$ to be WSSUS such that $R_{\mathbf{h}}(t_1,t_2,\tau_1,\tau_2) = P_{\mathbf{h}}(\Delta t,\tau_2)\delta(\tau_2-\tau_1)$, for some function $P_{\mathbf{h}}(\Delta t,\tau)$. Then, $R_{\mathbf{z}}(t_1,t_2)$ in (26) can be further simplified as follows:

$$\begin{aligned} R_{\mathbf{z}}(t_1,t_2) &= \iint P_{\mathbf{h}}(\Delta t,\tau_2)\delta(\tau_2-\tau_1)R_{\mathbf{u}}(\Delta t+\tau_1-\tau_2)d\tau_1 d\tau_2 \\ &= \int P_{\mathbf{h}}(\Delta t,\tau)R_{\mathbf{u}}(\Delta t)d\tau \\ &= R_{\mathbf{u}}(\Delta t)\int P_{\mathbf{h}}(\Delta t,\tau)d\tau \triangleq R_{\mathbf{z}}(\Delta t). \end{aligned} \tag{28}$$

The output $\mathbf{z}(t)$ is therefore WSS, and its PSD can be written as

$$\begin{aligned} \mathcal{S}_{\mathbf{z}}(f) &= \mathcal{F}_{\Delta t\to f}\{R_{\mathbf{z}}(\Delta t)\} \\ &= \mathcal{F}_{\Delta t\to f}\{R_{\mathbf{u}}(\Delta t)\} * \mathcal{F}_{\Delta t\to f}\left\{\int P_{\mathbf{h}}(\Delta t,\tau)d\tau\right\} \\ &= \mathcal{S}_{\mathbf{u}}(f) \overset{f}{*} \int P_{\mathrm{s}}(\nu,\tau)|_{\nu=f}d\tau, \end{aligned} \tag{29}$$

where $P_{\mathrm{s}}(\nu,\tau) \triangleq \mathcal{F}_{\Delta t\to\nu}\{P_{\mathbf{h}}(\Delta t,\tau)\}$ is known as the *scattering function* of the channel $\mathbf{h}(t,\tau)$. It provides a measure of the average power output of the channel as a function of the delay τ and the Doppler shift ν. Furthermore, if we define the *Doppler power spectrum* of the channel as $\mathcal{D}_{\mathbf{h}}(\nu) \triangleq \int P_{\mathrm{s}}(\nu,\tau)d\tau$, then (29) can be succinctly written as

$$\mathcal{S}_{\mathbf{z}}(f) = \mathcal{S}_{\mathbf{u}}(f) \overset{f}{*} \mathcal{D}_{\mathbf{h}}(\nu)|_{\nu=f}, \tag{30}$$

which is the result in Theorem 4.1, eq. (16).

From (30), we conclude that $\mathcal{S}_{\mathbf{z}}(f)$ depends on the *Doppler power spectrum* of the channel, $\int P_{\mathrm{s}}(\nu,\tau)d\tau$, but not on its *power delay profile* $\int P_{\mathrm{s}}(\nu,\tau)d\nu$. This is intuitively satisfying since all delayed replicas of the WSS process $\mathbf{u}(t)$ have the same PSD. Furthermore, if the channel $\mathbf{h}(t,\tau)$ is time-invariant, then $\mathcal{D}_{\mathbf{h}}(\nu) = \delta(\nu)$ and thus $\mathcal{S}_{\mathbf{z}}(f) = \mathcal{S}_{\mathbf{u}}(f)$, i.e., the channel does not affect the PSD of the input. On the other hand, if the channel is time-varying in such a way that it introduces a Doppler shift of f_0 Hz, then $\mathcal{D}_{\mathbf{h}}(\nu) = \delta(\nu - f_0)$ and thus $\mathcal{S}_{\mathbf{z}}(f) = \mathcal{S}_{\mathbf{u}}(f - f_0)$, i.e., the output PSD is simply the input PSD shifted by f_0 Hz, as expected.

Acknowledgements

The authors would like to thank L. A. Shepp, R. A. Scholtz, L. Greenstein, J. H. Winters, G. J. Foschini, M. Chiani, A. Giorgetti, and W. Suwansantisuk for their helpful suggestions.

REFERENCES

[1] E. Sousa, "Performance of a spread spectrum packet radio network link in a Poisson field of interferers," *IEEE Trans. Inf. Theory*, vol. 38, no. 6, pp. 1743–1754, 1992.

[2] J. Ilow, D. Hatzinakos, and A. Venetsanopoulos, "Performance of FH SS radio networks with interference modeled as a mixture of Gaussian and alpha-stable noise," *IEEE Trans. Commun.*, vol. 46, no. 4, pp. 509–520, 1998.

[3] X. Yang and A. Petropulu, "Co-channel interference modeling and analysis in a Poisson field of interferers in wireless communications," *IEEE Trans. Signal Process.*, vol. 51, no. 1, pp. 64–76, 2003.

[4] S. Govindasamy, F. Antic, D. Bliss, and D. Staelin, "The performance of linear multiple-antenna receivers with interferers distributed on a plane," in *Proc. IEEE Workshop on Signal Process. Advances in Wireless Commun.*, 2005, pp. 880–884.

[5] E. Salbaroli and A. Zanella, "A connectivity model for the analysis of a wireless ad hoc network in a circular area," in *Proc. IEEE Int. Conf. on Commun.*, June 2007, pp. 4937–4942.

[6] A. Giorgetti, M. Chiani, and M. Z. Win, "The effect of narrowband interference on wideband wireless communication systems," *IEEE Trans. Commun.*, vol. 53, no. 12, pp. 2139–2149, Dec. 2005.

[7] A. Giorgetti and D. Dardari, "The impact of OFDM interference on TH-PPM/BPAM transmission systems," in *Proc. IEEE Semiannual Veh. Technol. Conf.*, vol. 2, 2005, pp. 1037–1042.

[8] P. C. Pinto and M. Z. Win, "Communication in a Poisson field of interferers—part I: interference distribution and error probability," *IEEE Trans. Wireless Commun.*, vol. 9, no. 7, pp. 2176–2186, July 2010.

[9] M. Z. Win, P. C. Pinto, and L. A. Shepp, "A mathematical theory of network interference and its applications," *Proc. IEEE*, vol. 97, no. 2, pp. 205–230, Feb. 2009, special issue on Ultra-Wide Bandwidth (UWB) Technology & Emerging Applications.

[10] G. J. Foschini, "Private conversation," AT&T Labs-Research, May 2007.

[11] G. Samoradnitsky and M. Taqqu, *Stable Non-Gaussian Random Processes*. Chapman and Hall, 1994.

[12] D. Tse and P. Viswanath, *Fundamentals of Wireless Communication*. Cambridge University Press, 2005.

[13] J. Chambers, C. Mallows, and B. Stuck, "A method for simulating stable random variables," *J. Amer. Statist. Assoc.*, vol. 71, pp. 340–344, 1976.

[14] P. A. Bello, "Characterization of randomly time-variant linear channels," *IEEE Trans. Commun. Sys.*, vol. CS-11, no. 4, pp. 360–393, Dec. 1963.

[15] J. D. Parsons, *The Mobile Radio Propagation Channel*, 2nd ed. Wiley, 2000.

[16] R. Steele, *Mobile Radio Communications*. IEEE Press, 1992.

[17] J. Proakis, *Digital Communications*. McGraw-Hill, 2000.

[18] A. F. Molisch, *Wireless Communications*, 1st ed. IEEE Press, J. Wiley and Sons, 2005.

[19] P. C. Pinto and M. Z. Win, "Spectral characterization of wireless networks," *IEEE Wireless Commun. Mag.*, vol. 14, no. 6, pp. 27–31, Dec. 2007, special issue on Wireless Sensor Networking.

[20] A. Papoulis and S. U. Pillai, *Probability, Random Variables and Stochastic Processes*, 4th ed. McGraw-Hill, 2002.

[21] M. K. Simon, S. M. Hinedi, and W. C. Lindsey, *Digital Communication Techniques: Signal Design and Detection*, 1st ed. Prentice Hall, 1994.

[22] M. Z. Win, "On the power spectral density of digital pulse streams generated by M-ary cyclostationary sequences in the presence of stationary timing jitter," *IEEE Trans. Commun.*, vol. 46, no. 9, pp. 1135–1145, Sep. 1998.

[23] ——, "A unified spectral analysis of generalized time-hopping spread-spectrum signals in the presence of timing jitter," *IEEE J. Sel. Areas Commun.*, vol. 20, no. 9, pp. 1664–1676, Dec. 2002.

[24] D. P. Bertsekas and J. N. Tsitsiklis, *Introduction to Probability*. Athena Scientific, 2002.

Pedro C. Pinto (S'04) received the Licenciatura degree with highest honors in Electrical and Computer Engineering from the University of Porto, Portugal, in 2003. He received the M.S. degree in Electrical Engineering and Computer Science from the Massachusetts Institute of Technology (MIT) in 2006. Since 2004, he has been with the MIT Laboratory for Information and Decision Systems (LIDS), where he is now a Ph.D. candidate. His main research interests are in wireless communications and signal processing. He was the recipient of the MIT Claude E. Shannon Fellowship in 2007, the Best Student Paper Award at the IEEE International Conference on Ultra-Wideband in 2006, and the Infineon Technologies Award in 2003.

Moe Z. Win (S'85-M'87-SM'97-F'04) received both the Ph.D. in Electrical Engineering and M.S. in Applied Mathematics as a Presidential Fellow at the University of Southern California (USC) in 1998. He received an M.S. in Electrical Engineering from USC in 1989, and a B.S. (*magna cum laude*) in Electrical Engineering from Texas A&M University in 1987.

Dr. Win is an Associate Professor at the Massachusetts Institute of Technology (MIT). Prior to joining MIT, he was at AT&T Research Laboratories for five years and at the Jet Propulsion Laboratory for seven years. His research encompasses developing fundamental theory, designing algorithms, and conducting experimentation for a broad range of real-world problems. His current research topics include location-aware networks, time-varying channels, multiple antenna systems, ultra-wide bandwidth systems, optical transmission systems, and space communications systems.

Professor Win is an IEEE Distinguished Lecturer and elected Fellow of the IEEE, cited for "contributions to wideband wireless transmission." He was honored with the IEEE Eric E. Sumner Award (2006), an IEEE Technical Field Award for "pioneering contributions to ultra-wide band communications science and technology." Together with students and colleagues, his papers have received several awards including the IEEE Communications Society's Guglielmo Marconi Best Paper Award (2008) and the IEEE Antennas and Propagation Society's Sergei A. Schelkunoff Transactions Prize Paper Award (2003). His other recognitions include the Laurea Honoris Causa from the University of Ferrara, Italy (2008), the Technical Recognition Award of the IEEE ComSoc Radio Communications Committee (2008), Wireless Educator of the Year Award (2007), the Fulbright Foundation Senior Scholar Lecturing and Research Fellowship (2004), the U.S. Presidential Early Career Award for Scientists and Engineers (2004), the AIAA Young Aerospace Engineer of the Year (2004), and the Office of Naval Research Young Investigator Award (2003).

Professor Win has been actively involved in organizing and chairing a number of international conferences. He served as the Technical Program Chair for the IEEE Wireless Communications and Networking Conference in 2009, the IEEE Conference on Ultra Wideband in 2006, the IEEE Communication Theory Symposia of ICC-2004 and Globecom-2000, and the IEEE Conference on Ultra Wideband Systems and Technologies in 2002; Technical Program Vice-Chair for the IEEE International Conference on Communications in 2002; and the Tutorial Chair for ICC-2009 and the IEEE Semiannual International Vehicular Technology Conference in Fall 2001. He was the chair (2004-2006) and secretary (2002-2004) for the Radio Communications Committee of the IEEE Communications Society. Dr. Win is currently an Editor for IEEE TRANSACTIONS ON WIRELESS COMMUNICATIONS. He served as Area Editor for *Modulation and Signal Design* (2003-2006), Editor for Wideband Wireless and Diversity (2003-2006), and Editor for Equalization and Diversity (1998-2003), all for the IEEE TRANSACTIONS ON COMMUNICATIONS. He was Guest-Editor for the PROCEEDINGS OF THE IEEE (Special Issue on UWB Technology & Emerging Applications) in 2009 and IEEE JOURNAL ON SELECTED AREAS IN COMMUNICATIONS (Special Issue on Ultra -Wideband Radio in Multiaccess Wireless Communications) in 2002.